POST-TYPHOON ASSESSMENT OF SURFACE GREENNESS DISTURBANCE USING LANDSAT SERIES OBSERVATIONS

Feng Chen[1], Jonathan Li [1, 2], Cheng Wang[1]

[1] Fujian Key Laboratory of Sensing and Computing for Smart City, Xiamen University, Xiamen, China
[2] Department of Geography and Environmental Management, University of Waterloo, Waterloo, Canada

ABSTRACT

Extreme climate events are projected to increase under the context of global warming associated with the increase in greenhouse gas emissions. In particular, coastal regions which are also characterized with significant urbanization will be vulnerable to the extreme events, such as severe typhoon. Timely assessment and accurate information on the extent and severity of the damage caused by extreme event is necessary to better facilitate decision-making for disaster alleviation and post-recovery. Satellite remote sensing has an important advantage in assessing the impacts caused by extreme events on natural environment and socio-economic dimension at a variety of spatial and temporal scales. Surface greenness disturbance mainly over Xiamen, China, caused by Typhoon Meranti (2016) was investigated using a pair of observations by Landsat 7 ETM+ and Landsat 8 OLI. Significant decreases in greenness were detected, which mainly located along the Maluan Bay and the settlements in suburban and rural areas surrounding the track of typhoon.

Index Terms— Damage assessment, Typhoon Meranti, NDVI, Climate Data Records, Cross-comparison, Landsat, Surface reflectance

1. INTRODUCTION

At around 03:05 on September 15 (Beijing time, UTC+8), 2016, Meranti made landfall over the coastal regions of Xiang'an District, with the center position locating around (118.3°E, 24.5°N), Xiamen in Fujian Province, China, as a super typhoon with peak winds at the core about 48 m/s. It has been the strongest typhoon to ever making landfall in Fujian Province since 1949 (The Xinhua news agency). Most areas in Xiamen were heavily affected by Typhoon Meranti with significant damage to properties, and the direct economic losses were estimated about 10.2 billion RMB (about US$ 1.52 billion). Substantial damage to infrastructure and public services was also recorded. In particular, about 650 thousand trees planted along-side the streets got flattened after the landfall of Typhoon Meranti (http://www.xm.gov.cn). The damage to green covers possibly results in significant destruction of land surface ecosystem. By the way, during the 49th annual session of the ESCAP/WMO Typhoon Committee held in February 2017, the replacement of Meranti was approved, due mainly to its destructive power.

For post-risk assessment, the advantages of satellite remote sensing are always highlighted due to the easy availability and accessibility of data, especially the optical observations where large archives are often available (e.g. the Landsat archives), the relatively lower cost for observation with large extent, and the robustness and the efficiency of data processing techniques [7] [12]. To assess the damage to land surface ecosystem over Xiamen associated with Typhoon Meranti (2016), the changes in surface greenness between pre- and post- typhoon were investigated with the help of the Landsat series observations, including Landsat 7 Enhanced Thematic Mapper Plus (ETM+) and Landsat 8 Operational Land Imager (OLI).

2. DATA AND METHODS

Two Landsat observations (WRS-2 path/row: 119/43) acquired before and after the landfall of Typhoon Meranti (2016) over Xiamen were selected, in view of data quality and cloud cover, which included one observation by Landsat 8 OLI on 13 September and Landsat 7 ETM+ on 21 September 2016, respectively. In this paper, the higher level surface reflectance products (i.e. Surface Reflectance Higher Level Data Products) of Landsat were ordered through EarthExplorer (https://earthexplorer.usgs. gov/), whereas the data are processed and delivered from the ESPA On-Demand interface (https://espa.cr.usgs.gov/status/). By the way, currently, the Landsat surface reflectance products are available and can be ordered through EarthExplorer, which is updated with Collection 1 Higher-Level data sets (https://landsat.usgs.gov).

Normalized Difference Vegetation Index (NDVI, Eq. (1)) is a widely used indicator for mapping and monitoring vegetated areas using optical multi-spectral data. In this paper, NDVI was used to delineate both status and quantity of the surface greenness. Changes of land surface greenness caused by Typhoon Meranti were measured as the

differences/changes in NDVI between two observations (i.e. pre- and post-). This differencing approach is commonly used in the change detection between different image acquisitions. Similar methodology was used in damage assessments previously [8].

$$\mathrm{NDVI} = \frac{(\rho_{NIR} - \rho_{\mathrm{Red}})}{(\rho_{NIR} + \rho_{\mathrm{Red}})} \quad (1)$$

where ρ_{Red} and ρ_{NIR} refer to surface reflectance values of Band 3 and Band 4 in the Landsat 7 ETM+ sensor and Band 4 and Band 5 in the Landsat 8 OLI sensor, respectively.

Obvious variation or differences in sensor settings between the Landsat 8 OLI and its predecessors (e.g. the Landsat 7 ETM+) has been discussed [5] [13], which may cause significant between-sensors discrepancy in NDVI values [3] [6] [10]. Accordingly, an applicable transformation model is required to eliminate the between-sensors differences and to make the between-sensors comparison (i.e. differencing) available. A linear model used for transforming NDVI between Landsat 7 ETM+ and Landsat 8 OLI to facilitate cross-comparison of the two sensors is proposed in this paper, as shown in Fig. 1. The model is based on several spectra samples obtained from the ASTER Spectral Library Version 2.0 [2]. The spectra are provided in reflectance, and are available from http://speclib.jpl.nasa.gov. Related procedures and calculations for processing the spectra are detailed in [4], mainly include spectral interpolation and band effective reflectance.

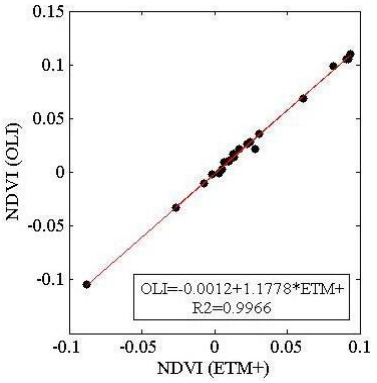

Fig. 1. Linear model for transforming NDVI between Landsat 8 OLI and Landsat 7 ETM+.

Therefore, the NDVIs obtained from the Landsat 7 ETM+ sensor were transformed to comparative values correspondingly as recorded by the Landsat 8 OLI sensor, through the linear model (Fig.1). Specifically, in this paper the changes of land surface greenness between pre- and post-typhoon were measured as the differences in NDVI between two acquisitions, which were calculated by subtracting the transformed NDVI of the Landsat 7 ETM+ (post-) from the NDVI recorded by Landsat 8 OLI (pre-).

3. RESULTS

A linear model with highly significant regressions (with R^2=0.9966 and p-value<0.0001) is obtained for the surface NDVI transformation between the Landsat 7 ETM+ and the Landsat 8 OLI, as shown in Fig. 1. It indicates that transformations between the Landsat 7 ETM+ NDVI and the Landsat 8 OLI NDVI are reliably obtained through the linear model, which shows accordance with the previous findings in [3]. However, in [3] the linear relationship was generated according to a very large collection of pixel samples from the corresponding Landsat 7 ETM+ and Landsat 8 OLI observations, which were located in the overlap of sensor acquisition pairs sensed one day apart. Sensitivity analysis of different transformation models is required in further investigations, although the linear model in Fig. 1 was used in this paper.

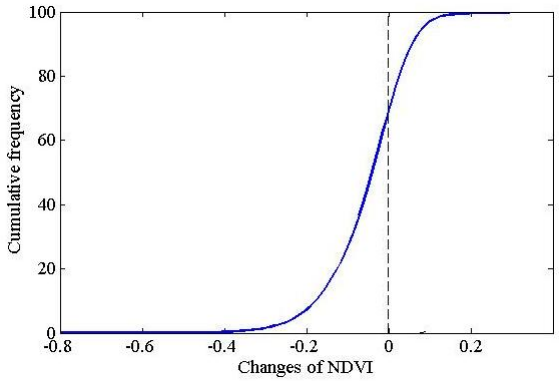

Fig. 2. General statistics of changes in greenness (NDVI) mainly over Xiamen after Typhoon Meranti (2016).

In general, about seventy percent of land surface covering the study area presented in Fig. 3 shows decrease trends in NDVI (Fig. 2) associated with Typhoon Meranti. Furthermore, areas with obvious NDVI decreases or extreme disturbance in surface greenness (with NDVI changing amplitude larger than 0.5) account for approximately ten percent. To demonstrate the damage intensity clearly, in Fig. 3, five categories are determined according to NDVI variation (the difference between post- and pre- Typhoon Meranti), specifically include “Normal”, “Low”, “Moderate”, “High”, and “Extreme”.By the way, many parts of records filled with invalid data are resulted from sensor faults of Landsat 7 ETM+ (e.g. the SLC problem and saturate of the ETM+ sensor) [4], cloud cover, and product processes. Accordingly, the land surface with invalid records or classified as water surface is labeled as “Undefined” (black color) in Fig. 3. Spatial variation in damage intensity is obvious (Fig. 3). Significant destructions are mainly located along coast region, especially the Maluan Bay, and the settlements in suburban and rural areas surrounding the track of typhoon (not shown) as well as in urban areas (e.g. Xiamen Island).

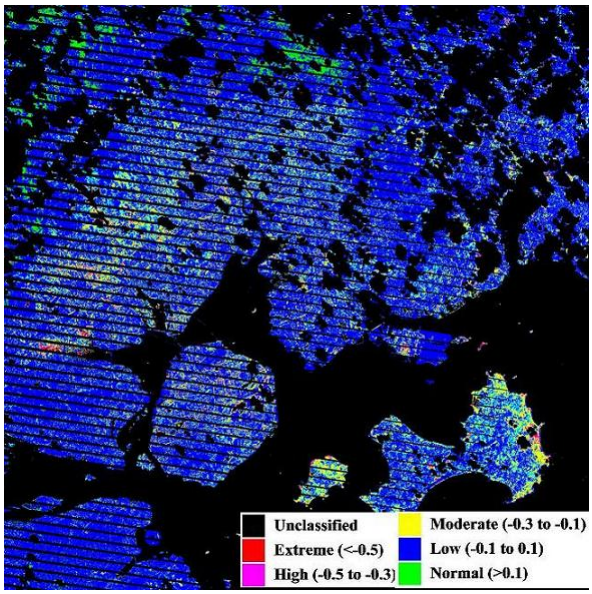

Fig. 3. Intensity of damage to land surface greenness mainly over Xiamen based on NDVI variation.

4. DISCUSSION AND CONCLUSIONS

Advantages of optical sensors are obvious for post-risk assessments [7] [11] [12], such as the Landsat 7 ETM+ and the Landsat 8 OLI discussed in this paper. Joint application of the observations by Landsat 7 ETM+ and Landsat 8 OLI provide more effective means for damage assessment, compared with the application using observations by one sensor of which the revisit interval is 16 days. Nevertheless, cloud cover always restricts the availability (number of observations and data quality) of valid observation during specific event (i.e. landfall of typhoon). For this reason, a Landsat 7 ETM+ observation taken approximately one week after the landfall of Typhoon Meranti (2016) was used in this study. The limited access to valid observations may result in uncertainties and ineffectiveness in post-risk assessments. To make up for the deficiency in valid observation of optical sensors, other data resources [1] and data integration or fusion are promising. General assessment of damage on regional surface greenness is obtained using the Landsat series observations; however, detailed investigations based on images with high spatial resolution should be done for specific managements [15]. To fully understand the damage to regional ecosystem, multi-scale observations both in spatial and temporal dimensions are beneficial [13] [14]. Currently, a coordination framework called "International Charter" has been operated, which aims to provide "a unified system of space data acquisition and delivery to those affected by natural or man-made disasters"
(https://www.disasterscharter.org/web/guest/home). With the help of the "International Charter", full advantages of all available earth observations will be taken to facilitate disaster related tasks, such as prediction, monitoring, assessment, and reconstruction.

Intensity of damage to land surface mainly over Xiamen associated with Typhoon Meranti (2016) was mapped according to the changes in NDVI (as surface greenness) recorded by a pair of Landsat observations. Areas affected significantly were shown thereby. Findings suggest that several settlements located around coast and in suburban and rural areas are more vulnerable to extreme events (i.e. Typhoon Meranti). However, to fully understand vulnerability and exposure to disaster (i.e. Typhoon), more case studies are extremely required, whereas only one case study was just shown in this paper. Mean while, to assess specific damages to urban area, more indicators covering other surface factors [9] and dimensions are useful.

In addition, the damage intensity was measured according to the decrease of NDVI through a differencing approach. Based on statistics of NDVI change, thresholds were selected, followed by the determination of damage levels. Careful threshold selection for the "damage" and "no-damage", and further of the damage levels is important. Accordingly, related ground truth and other information (e.g. words and pictures posted through social media) may benefit mapping validation.

5. ACKNOWLEDEMENT

This research was jointly supported by the National Key Research and Development Program of China (Grant 2016YFC1401001 and 2016YFC1401008) and China Postdoctoral Science Foundation. We thank the data providers for this investigation, including Dr. Simon Hook at NASA JPL and USGS, for the provision of the ASTER Spectral Library Version 2.0 and the Surface Reflectance Higher Level Data Products of Landsat archives, respectively.

6. REFERENCES

[1] A. D'Addabbo, A. Refice, G. Pasquariello, F.P. Lovergine, D. Capolongo, and S. Manfreda, "A Bayesian network for flood detection combining SAR imagery and ancillary data," *IEEE T. Geosci. Remote*, Piscataway, USA, vol. 54, no. 6, pp.3612-3625, 2016.

[2] A.M. Baldridge, S.J. Hook, C.I. Grove, and G. Rivera, "The ASTER spectral library version 2.0," *Remote Sens. Environ.*, Elsevier, New York, USA, vol. 113, pp. 711-715, 2009.

[3] D.P. Roy, V. Kovalskyy, H.K. Zhang, E.F. Vermote, L. Yan, S.S. Kumar, and A. Egorov, "Characterization of Landsat-7 to Landsat-8 reflective wavelength and normalized difference vegetation index continuity," *Remote Sens. Environ.*, Elsevier, New York, USA, vol. 185, pp. 57-70, 2016.

[4] F. Chen, L.N. Tang, C.P. Wang, and Q.Y. Qiu, "Recovering of the thermal band of Landsat 7 SLC-off ETM+ image using CBERS

as auxiliary data," *Adv. Space Res.*, Elsevier, Oxford, England, vol. 48, no. 6, pp. 1086-1093, 2011.

[5] F. Chen, S. Yang, Z. Su, and K. Wang, "Effect of emissivity uncertainty on surface temperature retrieval over urban areas: Investigations based on spectral libraries," *ISPRS J. Photogramm.*, Elsevier, Amsterdam, Netherlands, vol. 114, pp. 53-65, 2016.

[6] F. Chen, S. Yang, K. Yin, and P. Chan, "Challenges to quantitative applications of Landsat observations for the urban thermal environment," *J. Environ. Sci.-China*, Science China Press, Beijing, China, 2017. https://doi.org/10.1016/j.jes.2017.02.009

[7] M. Gianinetto, P. Villa, and G. Lechi, "Postflood damage evaluation using Landsat TM and ETM+ data integrated with DEM," *IEEE T. Geosci. Remote*, Piscataway, USA, vol. 44, no. 1, pp. 236-243, 2006.

[8] M.L. Bentley, T.L. Mote, and P. Thebepanya, "Using Landsat to identify thunderstorm damage in agricultural regions," *Bull. Amer. Meteorol. Soc*., AMS, Boston, USA, vol. 83, no. 3, pp. 363-376, 2002.

[9] M.A. Wagner, S.W, Mynit, and R.S, Cerveny. Geospatial assessment of recovery rates following a tornado disaster. *IEEE T. Geosci. Remote*, Piscataway, USA, pp.4313-4321, vol. 50, no.11, 2012.

[10] P. Li, L.G. Jiang, and Z.M. Feng, "Cross-comparison of vegetation indices derived from Landsat-7 Enhanced Thematic Mapper Plus (ETM+) and Landsat-8 Operational Land Imager (OLI) sensors," *Remote Sens.-Basel*, MDPI, Basel, Switzerland, vol. 6, pp.310-329, 2014.

[11] R. Negrón-Juárez, D.B. Baker, J.Q. Chambers, G.C. Hurtt, and S. Goosem, "Multi-scale sensitivity of Landsat and MODIS to forest disturbance associated with tropical cyclones," *Remote Sens. Environ.*, Elsevier, New York, USA, vol. 140, pp. 679-689, 2014.

[12] S.W. Myint, M. Yuan, R.S. Cerveny, and C. Giri, "Categorizing natural disaster damage assessment using satellite-based geospatial techniques," *Nat. Hazards Earth Syst. Sci.*, Copernicus Publications, Gottingen, Germany, vol. 8, pp. 707-719, 2008.

[13] T.R. Loveland and J.R. Irons, "Landsat 8: The plans, the reality, and the legacy," *Remote Sens. Environ.*, Elsevier, New York, USA, vol. 185, pp. 1-6, 2016.

[14] X.C. Li, L. Yu, Y.D. Xu, J. Yang, and P. Gong, "Ten years after Hurricane Katrina: monitoring recovery in New Orleans and the surrounding areas using remote sensing," *Sci. Bull*., Science China Press, Beijing, China, vol. 61, no. 18, pp.1460-1470, 2016.

[15] Z. Szantoi, S. Malone, F. Escobedo, O. Misas, S. Smith, and B. Dewitt, "A tool for rapid post-hurricane urban tree debris estimates using high resolution aerial imagery," *Int. J. Appl. Earth Obs.*, Elsevier, Amsterdam, Netherlands, vol. 18, pp. 548-556, 2012.